Available online at www.sciencedirect.com
SCIENCE DIRECT®
Journal of Power Sources 157 (2006) 98–103
JOURNAL OF POWER SOURCES
www.elsevier.com/locate/jpowsour

Effect of temperature on the mechanism of ethanol oxidation on carbon supported Pt, PtRu and Pt_3Sn electrocatalysts

Flavio Colmati, Ermete Antolini, Ernesto R. Gonzalez *

Instituto de Química de São Carlos, USP, C.P. 780, São Carlos, SP 13560-970, Brazil

Received 21 June 2005; accepted 20 July 2005
Available online 14 November 2005

Abstract

The electrochemical oxidation of ethanol on carbon supported Pt, PtRu and Pt_3Sn catalysts was studied in acid solutions at room temperature and in direct ethanol fuel cells (DEFC) in the temperature range 70–100 °C. In all the experiments, an enhancement of the activity for the ethanol oxidation was observed on the binary catalysts. In acid solution the improvement at low current densities was higher on PtRu than on Pt_3Sn. In DEFC tests, at 70 °C the cells with PtRu and Pt_3Sn showed about the same performance, while for $T > 70$ °C the cells with Pt_3Sn as anode material performed better than those with PtRu as anode material. The apparent activation energy for ethanol oxidation on PtRu catalyst was lower than on Pt_3Sn, particularly at high cell potentials, i.e. at low current densities. At low temperatures and/or low current densities, the positive effect of Ru oxides on the bifunctional mechanism determined the enhancement of activity for the ethanol oxidation reaction, while at high temperatures the positive effect of Sn alloying (enlarged lattice parameter) on CH_3CH_2OH adsorption and C–C cleavage prevails.

Keywords: Direct ethanol fuel cell; Ethanol oxidation; PtSn alloy; PtRu alloy

1. Introduction

The direct oxidation of methanol in fuel cells has been widely investigated. However, ethanol offers an attractive alternative as a fuel in low temperature fuel cells because it can be produced in large quantities from agricultural products and it is the major renewable biofuel from the fermentation of biomass. By comparing the performance of fuel cells employing an H_3PO_4-doped polybenzimidazole membrane and PtRu (4 mg cm^{-2}) as anode catalyst operating on various methanol-alternative fuels, Wang et al. [1] found that ethanol is a promising alternative fuel with an electrochemical activity comparable to that of methanol.

The goal of a number of studies carried out on the electrooxidation of ethanol was mainly to identify the adsorbed intermediates on the electrode and to elucidate the reaction mechanism by means of various techniques, such as differential electrochemical mass spectrometry (DEMS), in situ Fourier transform infrared spectroscopy (FTIRS) and electrochemical thermal desorption mass spectroscopy (ECTDMS) [2–7]. Much research effort in this area has been devoted to develop catalysts that avoid the auto-poisoning effect of adsorbed intermediate species formed in the ethanol oxidation reaction on platinum [1,3,6,8]. However, platinum alone is not a good catalyst for the ethanol oxidation reaction (EOR), and among others, PtRu and PtSn alloys have been identified as suitable materials [9–12]. The mechanism of ethanol oxidation in acid solution may be summarized in the following scheme of parallel reactions:

$$CH_3CH_2OH \rightarrow [CH_3CH_2OH]_{ad} \rightarrow C1_{ad},\ C2_{ad} \rightarrow CO_2\ \text{(total oxidation)} \quad (1)$$

$$CH_3CH_2OH \rightarrow [CH_3CH_2OH]_{ad} \rightarrow CH_3CHO \rightarrow CH_3COOH\ \text{(partial oxidation)} \quad (2)$$

in which ($C1_{ad}$ and $C2_{ad}$) represent the adsorbed intermediates on the electrode with one and two carbon atoms, respectively. Schmidt et al. [7] observed that the formation of chemisorbed species coming from dissolved ethanol is partially inhibited by the presence of Ru. This favours the oxidation pathway through weakly adsorbed species, and therefore, the selectivity for ethanal production was found to be higher compared to that on pure Pt. On the other hand, according to Fujiwara et al. [13], the promoter action of Ru seems to enhance the oxidation

* Corresponding author. Tel.: +55 16 3373 9899; fax: +55 16 3373 9952.
E-mail address: ernesto@iqsc.usp.br (E.R. Gonzalez).

0378-7753/$ – see front matter © 2005 Elsevier B.V. All rights reserved.
doi:10.1016/j.jpowsour.2005.07.087

of strongly bound intermediates (Eq. (1)) to give a higher relative yield of CO_2 than on pure Pt. According to Camara et al. [14], the dissociative adsorption of ethanol seems to be inhibited by Ru. Probably, this is due to the reduced number of neighbour Pt sites in the right configuration, which are necessary to adsorb the molecule and break the C–C bond.

According to Vigier et al. [15], in the case of the ethanol oxidation on Pt–Sn the presence of tin favours the dissociative adsorption of ethanol, which leads to the breaking of the C–C bond, at lower potentials and with a higher selectivity than on pure Pt.

Thus, although there is agreement that Pt–Sn and Pt–Ru are more active for the oxidation of ethanol, the effect of the second metal does not seem to be similar and more work is necessary to have a more clear picture of the limiting aspects of the reaction.

In this work, the electrochemical oxidation of ethanol on carbon supported Pt, PtRu and PtSn catalysts was studied in acid solution at room temperature and in direct ethanol fuel cells (DEFC) in the temperature range 70–100 °C.

The choice of the Pt–Sn and Pt–Ru atomic ratios used here was made on the basis of recent work on the ethanol oxidation reaction on these binary catalysts. Regarding Pt–Sn, Lamy et al. [16] observed the optimum Pt–Sn composition in the range 9:1–4:1, while Zhou et al. [17] found the optimum Pt–Sn composition in the range 2:1–3:2. On this basis, Pt–Sn in the atomic ratio 3:1 was chosen. In the case of Pt–Ru, Spinacé et al. [18] found that the activity for the ethanol oxidation increases with the increase of ruthenium contents (range investigated up to Pt–Ru 1:3). Oliveira Neto et al. [9] also observed that the activity for the oxidation of ethanol increases with the contents of the second metal (range investigated up to Pt–Ru 3:2). Camara et al. [14] found an optimum Pt–Ru composition of ca. 3:2. Here, a Pt–Ru atomic ratio 1:1 was selected.

2. Experimental

The following commercially available Pt-based fuel cell electrocatalysts were obtained from E-TEK (Natick, MA): 20 wt.% Pt supported on Vulcan XC-72 carbon black (Cabot Co), and Pt_3Sn and PtRu alloy electrocatalysts, also 20 wt.% metal on Vulcan XC-72 (Cabot) carbon black with nominal stoichiometries of 25 at.% Sn and 50 at.% Ru.

X-ray diffractograms of the catalysts were obtained in a universal diffractometer Carl Zeiss-Jena, URD-6, operating with Cu Kα radiation ($\lambda = 0.15406$ nm) generated at 40 kV and 20 mA. Scans were done at 3° min^{-1} for 2θ values between 30° and 100°. In order to estimate the particle size from XRD, Scherrer's equation [19] was used. For this purpose, the (2 2 0) peak of the Pt fcc structure around $2\theta = 70°$ was selected. In order to improve the fitting of the peak, recordings for 2θ values from 60° to 80° were done at 0.02° min^{-1}.

In order to test the electrochemical behaviour in a single DEFC fed with ethanol solution/oxygen, the electrocatalysts were used to make two layer gas diffusion electrodes (GDE). A diffusion layer was made with carbon powder (Vulcan XC-72) and 15 wt.% (w/w) PTFE and applied over a carbon cloth (PWB-3, Stackpole). On top of this layer, the electrocatalyst was applied in the form of a homogeneous dispersion of Pt_3Sn/C, PtRu/C or Pt/C, Nafion® solution (5 wt.%, Aldrich) and isopropanol (Merck). All electrodes were made to contain 1 mg Pt cm^{-2}.

To build the membrane and electrode assembly (MEA), two GDEs were hot pressed on both sides of a Nafion® 115 membrane at 125 °C and 50 kg cm^{-2} for 2 min. Before use, the Nafion® membranes were treated with a 3 wt.% solution of H_2O_2, washed and then treated with a 0.5 mol L^{-1} H_2SO_4 solution. The geometric area of the electrodes was 4.62 cm^2. In the DEFC studies, Pt_3Sn/C or PtRu/C were used as active anode materials and 20 wt.% Pt/C as cathode material. The cell polarization data at 3 atm O_2 pressure and in the temperature range 70–100 °C were obtained by circulating at the anode a 1 mol L^{-1} aqueous ethanol solution.

The CO stripping experiments were carried out in a single cell in which the cathode was fed with hydrogen, serving as counter and reference electrode. The following procedures were applied to the anode side: after recording a CV in a N_2 purged system, CO was admitted to the cell and adsorbed at 0.075 V for 20 min. The excess CO was eliminated with N_2 gas and the stripping charges determined between 0.075 and 1.0 V versus a RHE, using a 10 mV s^{-1} scan rate, after correcting the currents for the background. Linear sweep voltammograms were recorded in the range 0.1–0.8 V versus a RHE. The oxidation of ethanol on Pt/C, Pt_3Sn/C and PtRu/C was tested in a similar system, but instead of CO a 1 mol L^{-1} ethanol solution was fed to the anode side. The experiments were done at room temperature with a 1285 A Solartron Potentiostat connected to a personal computer and using the software CorrWare for Windows (Scribner).

3. Results and discussion

Fig. 1 shows the XRD patterns of the carbon-supported Pt, Pt_3Sn and PtRu catalysts. All the XRD patterns clearly show the main characteristic peaks of the face-centered cubic (fcc) crystalline Pt, showing that all the alloy catalysts resemble the single-phase disordered structure (solid solution). The diffraction peaks of the binary alloy catalysts are shifted to lower 2θ

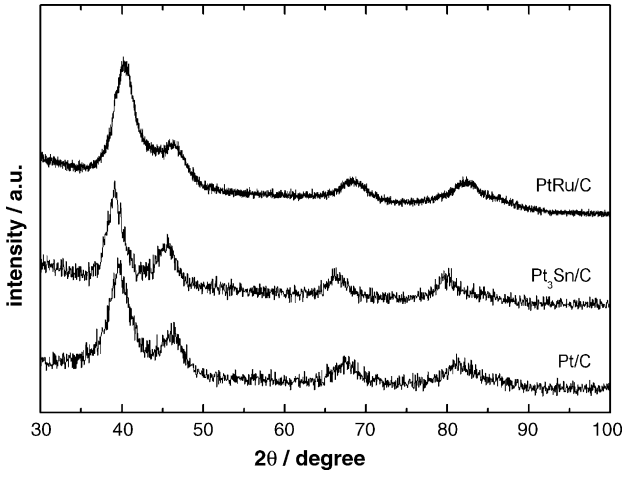

Fig. 1. XRD diffractograms of carbon supported 20 wt.% Pt, Pt_3Sn and PtRu alloy catalysts.

Table 1
Lattice parameters and metal particle sizes for Pt/C, PtRu/C and Pt_3Sn/C catalysts

Catalyst	Lattice parameter (nm)	Metal particle size (nm)
Pt/C	0.39155	2.9
PtRu/C	0.38868	3.2
Pt_3Sn/C	0.40015	4.1

values in the case of Pt_3Sn, and to higher 2θ values in the case of PtRu with respect to the corresponding peaks in pure Pt. The 2θ angle shifts of the Pt peaks reveal alloy formation between Pt and Sn or Ru, caused by the incorporation of the base metal in the fcc structure of Pt. No peaks for pure Sn or Ru and/or their oxides were found, but their presence cannot be discarded because they may be present in a small amount or even in an amorphous form. The lattice parameters of all the catalysts are given in Table 1. The lattice parameter for the PtRu alloy catalyst is smaller than that of Pt, indicating a contraction of the lattice after alloying, while the lattice parameter of Pt_3Sn catalyst is larger than that of pure Pt, due to a lattice expansion after alloying. In the case of the Pt_3Sn alloy catalyst the value of the lattice parameter is in agreement with that for the bulk Pt_3Sn solid solution (0.400 nm [20]), indicating a high degree of alloying. Then, it can be deduced that the amount of metal oxide species in this material is very small. For the PtRu alloy catalyst, instead, the value of the lattice parameter is remarkably larger than those for the bulk PtRu solid solution (0.38636 nm [21]) or for carbon supported PtRu (0.38535 nm), calculated on the basis of the relation reported in Ref. [22]. This indicates a low degree of alloying, and, as a consequence, the presence of non-alloyed Ru and/or its oxides.

The average size of the Pt, Pt_3Sn and PtRu alloy nanoparticles was estimated from the XRD (2 2 0) peak by using Scherrer's equation [19]:

$$d = \frac{0.9k1}{B_{(2)}} \cos\theta \quad (3)$$

where d is the average particle diameter, k_1 the wavelength of X-ray radiation (0.154056 nm), θ the angle of the (2 2 0) peak, and $B_{(2)}$ is the width in radians of the diffraction peak at half height. In order to obtain better values of $B_{(2)}$ the (2 2 0) peak was fitted with a gaussian function. The obtained average particle sizes of all the catalysts are given in Table 1. As can be seen, the particle size of the Sn-containing catalyst is larger than those of Pt and PtRu.

Fig. 2 shows CO stripping voltammograms for the Pt/C, Pt_3Sn/C and PtRu/C catalysts recorded at 10 mV s^{-1} in the supporting electrolyte at room temperature. On Pt, the onset of CO oxidation is close to 680 mV versus RHE and the maximum of the oxidation peak occurs at 750 mV versus RHE. For both Pt_3Sn and PtRu, the onset of CO oxidation occurs at lower potentials than on Pt, i.e. close to 400 mV versus RHE, while the maximum of the peak is located at 650 mV versus RHE for Pt_3Sn, and at 590 mV versus RHE for PtRu. The negative shift observed in the stripping voltammograms for the catalysts containing Sn or Ru is in agreement with data reported by Morimoto and Yeager

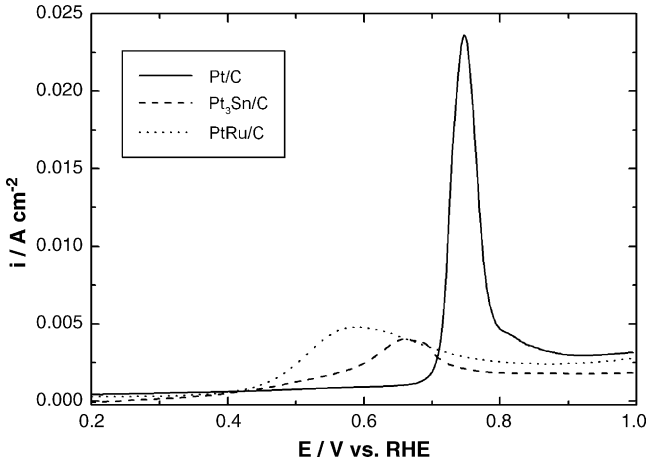

Fig. 2. Stripping voltammograms of adsorbed CO on Pt/C, Pt_3Sn/C and PtRu/C electrocatalysts recorded at 10 mV s^{-1}.

[23] and Wang et al. [24] for PtSn and Dinh et al. [25] and Cao and Bergens [26] for PtRu. The shift of potential to less positive values on the Pt_3Sn and PtRu catalysts is attributed to the presence of oxygenated species on Sn and Ru sites formed at lower potentials in comparison with platinum. According to the bifunctional mechanism [27], these oxygenated species allow the oxidation of CO to CO_2 at lower potentials. Fig. 2 shows that the shape and position of the CO stripping peak depends largely on the nature of the catalyst. On the basis of only the bifunctional mechanisms, it must be concluded that the formation of oxygenated species require lower potentials for PtRu than for Pt_3Sn. The oxidation of adsorbed CO occurs over a relatively large potential range on Pt_3Sn and PtRu in comparison with Pt, where the adsorbed CO is oxidized in a narrow current peak.

Fig. 3 shows the linear sweep voltammograms for ethanol oxidation at room temperature on Pt/C, Pt_3Sn/C and PtRu/C catalysts. With Ru, the electrocatalytic activity observed is greatly enhanced mainly at low potentials. A smaller enhancement is also observed for the catalysts with Sn in comparison to pure platinum. The current for ethanol oxidation on PtRu increases

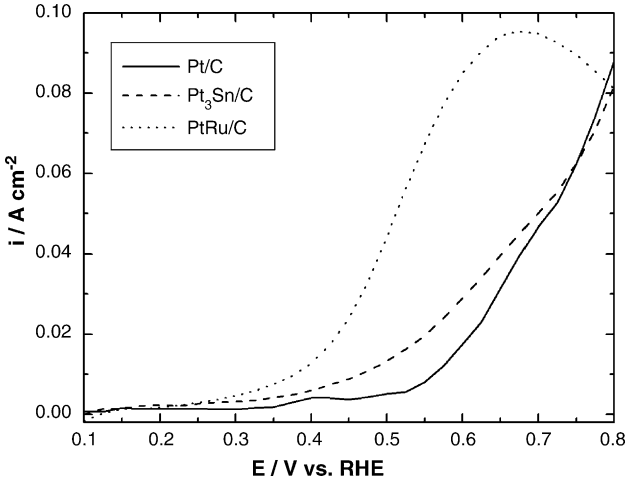

Fig. 3. Linear sweep voltammograms for ethanol oxidation on Pt/C, Pt_3Sn/C and PtRu/C electrocatalysts obtained in the single cell, circulating a 1.0 mol L^{-1} ethanol solution at 1 mL min^{-1}.

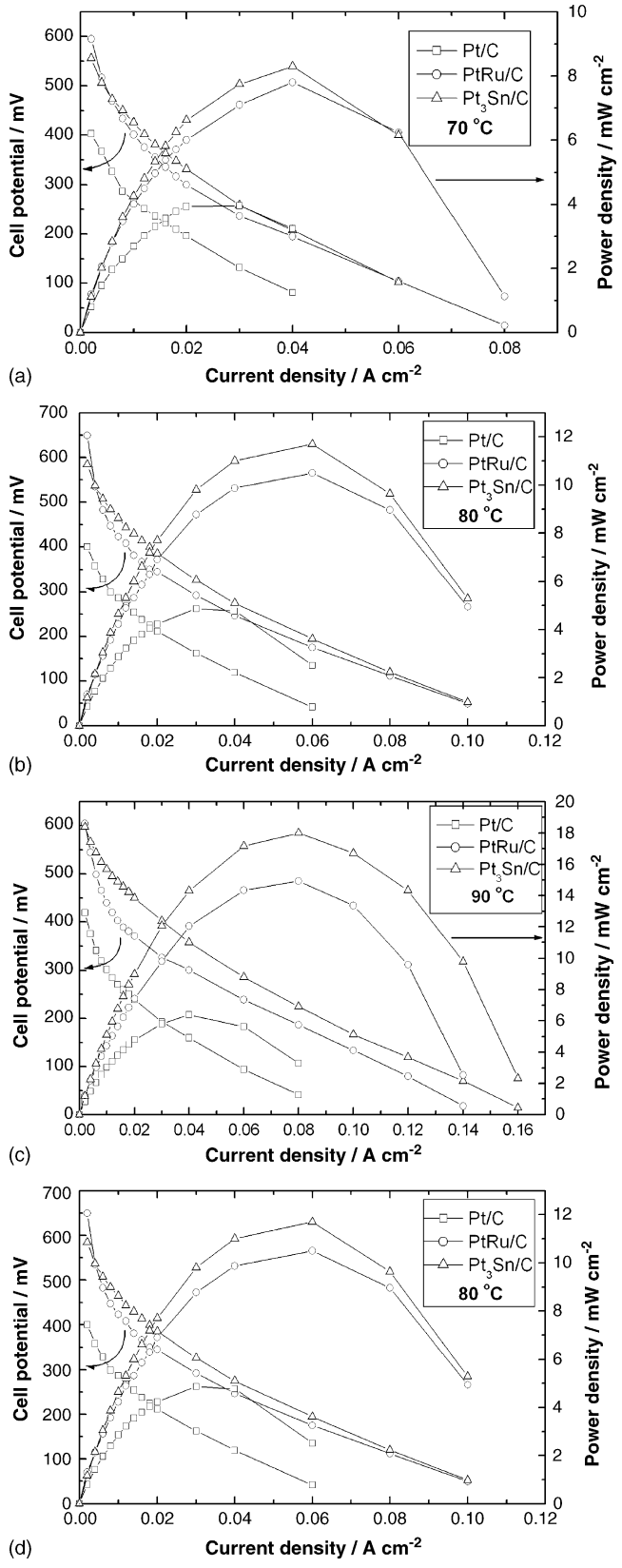

Fig. 4. Potential–current density curves and power density–current density curves in single direct ethanol fuel cells with Pt/C, Pt_3Sn/C and PtRu/C as anode electrocatalysts for ethanol oxidation at (a) 70 °C, (b) 80 °C, (c) 90 °C and (d) 100 °C, and 3 atm O_2 pressure using a 1 mol L^{-1} ethanol solution. Anode metal loading: 1 mg cm^{-2}. Cathode 20 wt.% Pt/C, Pt loading 1 mg cm^{-2}.

sharply in going from 400 to 600 mV, while the increase of the oxidation current on Pt_3Sn and Pt is small until the potential exceeds 600 mV. The same shape of the *j*/*E* curve for PtRu was observed by Lamy et al. [16] for non-alloyed Pt_9Sn prepared by Bonneman's method and by Colmati et al. [28] for partially alloyed Pt_3Sn and Pt_2Sn prepared by reduction with formic acid. In all these cases, the presence or the formation because as previously mentioned a negligible amount of oxide is present in Pt_3Sn, of oxygenated species on the surface of the catalysts can supply oxygen-containing species for the oxidative removal of CO and CH_3CO species [15] adsorbed on adjacent Pt active sites, enhancing in this way the ethanol electro-oxidation activity at low potentials. Contrary to the results of the present work, Lamy et al. [16] observed a poor activity of Pt_4Ru for the oxidation of ethanol at room temperature. According to Camara et al. [14], there is a relatively narrow range of Pt–Ru compositions that present a high activity for ethanol oxidation: for a Ru content lower than 20 at.%, there are not enough Ru sites to effectively assist the oxidation of adsorbed intermediates and the oxidation current remains at the low levels observed for pure Pt. The low Ru content could explain the poor activity of the Pt_4Ru catalyst observed by Lamy et al. [16]. According to the results in Fig. 3, the onset potentials for ethanol oxidation were ca. 270 mV on PtRu, 300 mV on Pt_3Sn and 375 mV on Pt, in the same order observed by Zhou et al. [29].

The results obtained in the direct ethanol fuel cell in terms of potential–current density curves and power density–current density curves for Pt/C, Pt_3Sn/C and PtRu/C at 70, 80, 90 and 110 °C are shown in Fig. 4a–d, respectively. When Pt/C was used as anode catalyst, the single cell exhibited a poor performance at all temperatures. When Pt_3Sn or PtRu catalysts were used in the anode, a remarkable enhancement in the cell performance was observed. Pt_3Sn performed better than PtRu, and the difference increased with increasing operating temperature of the cell. This result is very interesting because it shows that the higher activity of PtRu at lower potentials observed in the CVs at room temperature (cf. Fig. 3) is not confirmed in the experiments under the operational conditions in single cells. By plotting the maximum

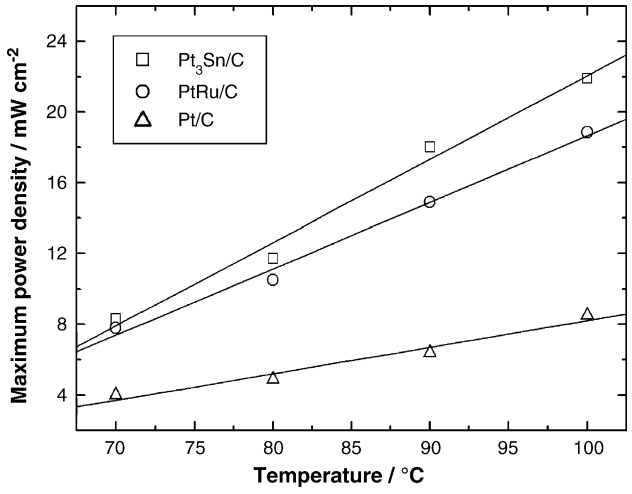

Fig. 5. Dependence of the maximum power density on cell temperature for single cells with Pt/C, Pt_3Sn/C and PtRu/C as anode electrocatalysts.

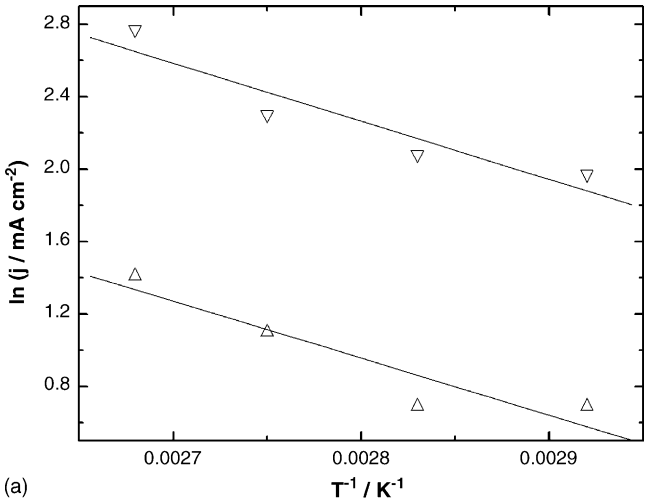

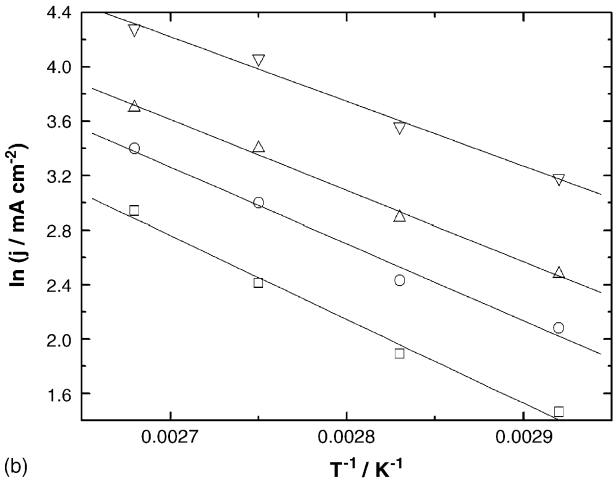

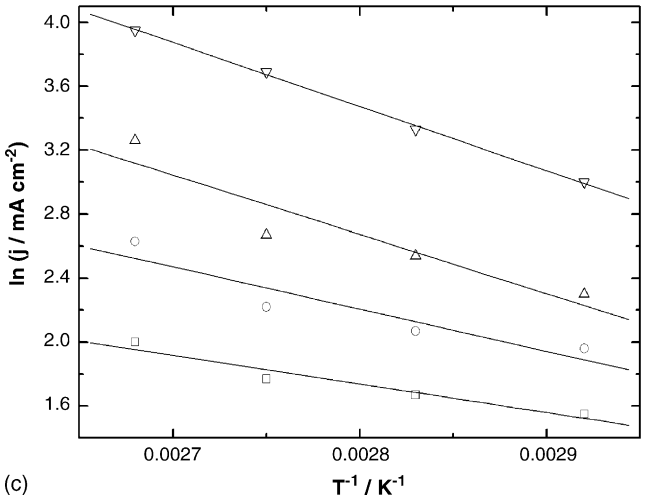

Fig. 6. Arrhenius plots for (a) Pt/C, (b) Pt_3Sn/C and (c) PtRu/C in direct ethanol fuel cells at various potentials. (▽) 300 mV; (△) 400 mV; (◯) 450 mV; (□) 500 mV.

power density versus cell temperature a linear dependence was obtained for all the catalysts, as shown in Fig. 5. The slope of the lines increases in the order Pt < PtRu < Pt_3Sn, indicative of differences in the activation energy for the reaction. The apparent activation energies for ethanol oxidation on the Pt, Pt_3Sn and PtRu catalysts were obtained at different potentials by linear regression of the Arrhenius plots presented in Figs. 6a–c, and were all potential dependent. The E_a for ethanol oxidation on Pt_3Sn was higher than that on PtRu for all the potentials investigated.

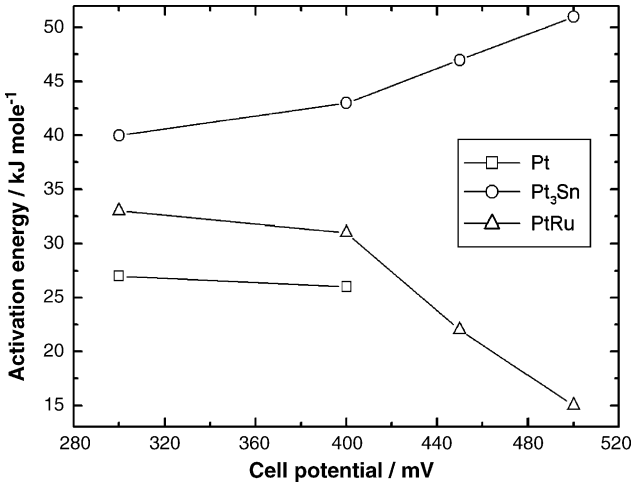

Fig. 7. Dependence of the apparent activation energy on cell potential.

The values of the activation energy are plotted versus the cell potential in Fig. 7. For the PtRu catalyst, E_a decreases with increasing cell potentials, in the same way as the dependence of E_a on potential for methanol oxidation found by Jang and Kucernak [30]. On the other hand, and contrary to what was observed for PtRu, the activation energy for ethanol oxidation on PtSn increases with increasing cell potentials. In the same way as for methanol oxidation [31], the larger value of E_a for ethanol oxidation on Pt_3Sn could indicate that the rate determining step is the adsorption step, whereas the lower activation energy on PtRu suggests that the reaction is diffusion controlled.

At low temperatures Ru and Sn favour the formation of CO_2 and CH_3COOH at lower potentials more than Pt through the oxidation of adsorbed CO and CH_3CO species, respectively, according to the bifunctional mechanism. In the case of PtRu, this positive effect of Ru is enhanced by the presence of ruthenium oxide.

At high temperatures and lower potentials (high current densities), the dissociative adsorption of ethanol on Pt_3Sn is enhanced and may take place at lower potentials than on PtRu or Pt. The presence of alloyed tin, expanding the lattice allows ethanol to adsorb and dissociate, with breaking of the C–C bond, at lower potentials than on PtRu and pure Pt.

4. Conclusions

The effect of Ru and Sn on PtRu and Pt_3Sn catalysts is to increase the rate of ethanol oxidation both at low and high temperatures with respect to pure Pt.

At low temperatures the activity for ethanol oxidation is higher on PtRu than on Pt_3Sn, while at high temperatures the cell with Pt_3Sn performed better than that with PtRu.

The apparent activation energy for ethanol oxidation on Pt_3Sn is higher than that on PtRu at all the investigated potentials, which indicates differences in the reaction mechanism.

At low temperatures the oxidation of adsorbed CO and CH_3CO species on PtRu is enhanced by the positive effect of the presence of ruthenium oxide through the bifunctional mechanism.

At high temperatures and high current densities the presence of alloyed tin, expanding the lattice, allows ethanol to adsorb dissociatively, with breaking of the C–C bond, at lower potentials than on pure Pt and on PtRu.

Acknowledgements

The authors thank the Conselho Nacional de Desenvolvimento Científico e Tecnológico (CNPq, Proc. 142266/2003-5) and the Fundação de Amparo a Pesquisa do Estado de São Paulo (FAPESP, Proc. 99/06430-8 and Proc. 03/04334-9) for financial support.

References

[1] J. Wang, S. Wasmus, R.F. Savinell, J. Electrochem. Soc. 142 (1995) 4218.
[2] J. Willsau, J. Heitbaum, J. Electroanal. Chem. 194 (1985) 27.
[3] T. Iwasita, E. Pastor, Electrochim. Acta 39 (1994) 531.
[4] B. Bittins-Cattaneo, S. Wilhelm, E. Cattaneo, H.W. Buschmann, W. Vielstich, Ber. Bunsenges. Phys. Chem. 92 (1988) 1210.
[5] H. Hitmi, E.M. Belgsir, J.-M. Leger, C. Lamy, R.O. Lezna, Electrochim. Acta 39 (1994) 407.
[6] J.F.E. Gootzen, W. Visscher, J.A.R. Van Veen, Langmuir 12 (1996) 5076.
[7] V.M. Schmidt, R. Ianniello, E. Pastor, S. Gonzalez, J. Phys. Chem. 100 (1996) 17901.
[8] A.V. Tripkovic, K.Dj. Popovic, J.D. Lovic, Electrochim. Acta 46 (2001) 3163.
[9] A. Oliveira Neto, M.J. Giz, J. Perez, E.A. Ticianelli, E.R. Gonzalez, J. Electrochem. Soc. 149 (2002) A272.
[10] E.V. Spinacé, A. Oliveira Neto, M. Linardi, J. Power Sources 129 (2004) 121.
[11] W. Zhou, Z. Zhou, S. Song, W. Li, G. Sun, P. Tsiakaras, Q. Xin, Appl. Catal. B 46 (2003) 273.
[12] C. Lamy, E.M. Belgsir, J.-M. Leger, J. Appl. Electrochem. 31 (2001) 799.
[13] N. Fujiwara, K.A. Friedrich, U. Stimming, J. Electroanal. Chem. 472 (1999) 720.
[14] G.A. Camara, R.B. de Lima, T. Iwasita, Electrochem. Commun. 6 (2004) 812.
[15] F. Vigier, C. Coutanceau, F. Hahn, E.M. Belgsir, C. Lamy, J. Electroanal. Chem. 563 (2004) 81.
[16] C. Lamy, S. Rousseau, E.M. Belgsir, C. Coutanceau, J.-M. Léger, Electrochim. Acta 49 (2004) 3901.
[17] W.J. Zhou, S.Q. Song, W.Z. Li, Z.H. Zhou, G.Q. Sun, Q. Xin, S. Douvartzides, P. Tsiakaras, J. Power Sources 140 (2005) 50.
[18] E.V. Spinacé, A. Oliveira Neto, T.R.R. Vasconcelos, M. Linardi, J. Power Sources 137 (2004) 17.
[19] B.E. Warren, X-Ray Diffraction, Addison-Wesley, Reading, MA, 1969.
[20] M. Hoheisel, S. Speller, J. Kuntze, A. Atrei, U. Bardi, W. Heiland, Phys. Rev. B 63 (2001) 245403.
[21] D. Chu, S. Gilman, J. Electrochem. Soc. 143 (1996) 1685.
[22] E. Antolini, F. Cardellini, J. Alloy Compd. 315 (2001) 118.
[23] Y. Morimoto, E.B. Yeager, J. Electroanal. Chem. 441 (1998) 77.
[24] K. Wang, H.A. Gasteiger, N.M. Markovic, P.N. Ross, Electrochim. Acta 41 (1996) 2587.
[25] H.N. Dinh, X. Ren, F.H. Garzon, P. Zelenay, S. Gottesfeld, J. Electroanal. Chem. 491 (2000) 222.
[26] D. Cao, S.H. Bergens, Electrochim. Acta 48 (2003) 4021.
[27] M. Watanabe, S. Motoo, J. Electroanal. Chem. 60 (1975) 275.
[28] F. Colmati, E. Antolini, E.R. Gonzalez, J. Electroanal. Chem., submitted for publication.
[29] W.J. Zhou, B. Zhou, W.Z. Li, Z.H. Zhou, S.Q. Song, G.Q. Sun, Q. Xin, S. Douvartzides, M. Goula, P. Tsiakaras, J. Power Sources 126 (2004) 16.
[30] J. Jiang, A. Kucernak, J. Electroanal. Chem. 543 (2003) 187.
[31] F. Fiçicioglu, F. Kardigan, J. Electroanal. Chem. 430 (1997) 179.